J. Fluid Mech. (1982), *vol.* 115, *pp.* 395–410
Printed in Great Britain

On the steady-state relations between disturbances above and below a critical level

By E. W. GRAHAM
Graham Associates, Shaw Island, WA 98286

(Received 5 January 1981 and in revised form 18 May 1981)

In studying the behaviour of a density-stratified shear flow difficulties are encountered at the 'critical' level where wave velocity equals fluid velocity.

Here a stratified shear layer of finite thickness is considered and a two-dimensional nonlinear steady-state problem is studied. It is assumed that blocking creates separate pockets of trapped fluid, each mixed to uniform density. These pockets are not in static equilibrium with the surrounding stratified fluid. They must be supported either by pressures dynamically developed in the curved flow along continuous streamlines outside the pockets or by centrifugal forces resulting from circulation within the pockets. The latter effect is considered only through evaluation of a crude 'factor of importance', F_R, for the rotational effects and the pockets are assumed to be stagnant in the primary analysis.

For small but finite disturbance amplitude F_R approaches zero, indicating that no correction of the primary analysis is required. A limiting Richardson number of unity appears. Above this limit the primary analysis gives no solutions and apparently the separate pockets of stagnant fluid merge to form a continuous stagnant insulating layer. This behaviour of the critical level (as a barrier to communication) resembles earlier results from transient linearized investigations although the two analyses have little in common except the existence of a critical level separating two fluid regions.

For moderate-to-large disturbance amplitudes the geometry of the flow pattern suggests Kelvin–Helmholtz billows. Rotational effects increase as the amplitude increases and may become significant at this stage. The primary analysis then becomes less accurate and cannot be used to exclude Kelvin–Helmholtz billows at Richardson numbers somewhat greater than unity.

1. Introduction

Preliminary remarks

Internal waves in the ocean exist because of small variations of density in the vertical direction, just as surface waves exist because of the large density difference between water and the air above. In each case vertical displacement of the fluid creates a restoring force, small for internal waves and large for surface waves. For internal waves the period is large (e.g. 10 minutes) and the horizontal propagation velocity small.

Because of the low horizontal velocities of the internal waves they can be seriously affected by variations of a few feet per second in horizontal fluid velocity. Variation of the horizontal fluid velocity with depth is called vertical shear. A particularly

interesting and difficult problem arises when wave velocity is equal to fluid velocity at some height (the critical level) in the shear layer.

The present study is an attempt to determine what relation exists in the steady state between disturbances above and below a critical level.

Previous work

The steady-state flow pattern we seek might be thought of as the end result of some transient process related to (but not identical with) that investigated by Booker & Bretherton (1967). On the other hand, for moderately large amplitude the geometry of the flow pattern resembles a row of Kelvin–Helmholtz billows. Thus two lines of comparison are suggested.

Pursuing the first line, we note a few of the many contributions in this field. Bretherton (1966) and Booker & Bretherton (1967) showed the absorption of infinitesimal transient internal waves near the critical level. Their mathematical analysis was based on the work of Miles (1961), who showed the relation between solutions above and below the singular point (critical height) for the linearized equations. Hines & Reddy (1966) indicated an energy absorption in this region but by a different mechanism.

Pursuing the second line of comparison, we note some examples of work related to Kelvin–Helmholtz billows. Kelly & Maslowe (1970) considered a nonlinear steady-state problem for small Richardson numbers, and Maslowe (1972, 1973) extended this to larger Richardson numbers. Margolis & Su (1978) also studied a nonlinear steady-state problem, but where Maslowe accounted for some effects of recirculation they considered the fluid in the pockets as static. In spite of this difference, solutions were obtained for Richardson numbers greater than unity in both references. Our rather primitive analysis suggests that solutions for $R > 1$ are possible only if recirculation effects are included.

Margolis and Su remarked on the non-uniqueness of the solutions and this is also observable in our results.

Mollo-Christensen (1978) investigated a continuous layer of fluid trapped between two sets of Gerstner waves, one on the fluid below and the other on the fluid above. These Gerstner waves were assumed to be moving at the same velocity so that the intervening fluid layer was stagnant with respect to co-ordinates moving at wave speed. From our point of view this continuous stagnant layer prevents communication between the regions above and below, and the synchronization of upper and lower waves might require further explanation.

Assumptions and discussion

We see the essential feature of these two-dimensional stratified shear flows as blocking† in the region where fluid velocities are small relative to the internal wave (i.e. near the critical level). Any disturbance must displace streamlines, and such displacements (either up or down) require additional potential energy (because of density stratification). In steady flow this might be obtained by conversion of kinetic energy, but near the zero-velocity streamline there is very little kinetic energy available. Streamlines near the critical level are therefore blocked in steady flow. This fluid is assumed to be trapped in pockets which appear periodically in the horizontal direction. For simplicity

† The validity of this assumption remains to be determined.

this fluid is taken as completely mixed and essentially stagnant. Periodicity is assumed but phase and amplitude variations between the upper and lower flow patterns are permitted.

For stagnant fluid in the pockets there must be velocity discontinuities across the boundaries of the pockets. Actually viscous forces will create a rotation within the pocket and the corresponding centrifugal forces might affect the analysis. A crude estimate of the importance of such effects (described later) indicates that they are negligible for small ratios of amplitude to wavelength and of only secondary importance for moderately large ratios.

It has also been suggested by a referee that the stagnant-pocket assumption might apply to billows which have recently been formed by the breaking of Kelvin–Helmholtz waves (i.e. before there has been sufficient time for the viscous forces to establish significant rotation in the pockets; see for example Benney & Ko (1978, p. 198)).

Two functions, $f_1(\rho)$ and $f_2(\rho)$, are used later to characterize the stream tubes in the steady state. One might assume that initially there exists a shear layer infinitely long in the flow direction. This shear layer is then disturbed over some finite length sufficient to contain several wavelengths. In this disturbed region separate pockets are formed. Beyond the disturbed region the blocking creates a continuous nearly stagnant layer containing the critical level. This layer tends to prevent communication between the lower and upper fluid so that each may be said to have its own upstream direction. If the functions $f_1(\rho), f_2(\rho)$ are altered in the disturbed region they must also be altered infinitely far upstream. We assume that this remote upstream effect does not exist except within the blocked thickness of the shear layer. Therefore the functions of ρ are taken to be unchanged for ρ values outside of the blocked thickness. Such arguments are of course to some extent heuristic.

The stagnant regions are studied first. They are considered to be bounded by sinusoidal curves. The velocity and pressure distribution are determined along the upper and lower streamlines that bound the stagnant region. (The velocity and density boundary layers which must actually separate fluid in the pocket from the external flow are omitted here.) Blocking is presumed to extend only through that portion of the shear layer where complete streamlines (from plus to minus infinity) cannot be formed. Hence it would be desirable to require a true stagnation point on each boundary streamline. However, to avoid difficulties in the numerical analysis points of very low velocity are specified instead.†

The volume of stagnant fluid in a 'pocket' is taken to be exactly that which is contained between the upper- and lower-boundary streamlines in the same length of the undisturbed flow. This implies that the creation of the disturbed flow field did not involve large-scale transport of fluid such as would appear if the two boundary streamlines were on the average moved closer together or farther apart. The stagnant region is assumed to be entirely in the shear layer.

Step-by-step construction of further streamlines is accomplished numerically until the outer edges of the finite-thickness shear layer are reached. There we attempt to match streamline shape and velocity approximately with potential flow fields or replace the streamline with a solid boundary.

A difficult and important factor not considered here is flow-pattern stability.

† In spite of this precaution there are inaccuracies in the $\bar{x}$-interval 0 to $\frac{1}{8}\pi$.

2. Outline of analysis

The analysis begins with the study of pressure distribution in a stagnant region of simple shape, existing in a shear layer which, in the undisturbed condition, had linear density and velocity variations with depth.

This analysis alone yields some interesting restrictions on Richardson number, but we need to know whether or not the local pattern is compatible with any useful upper-boundary conditions, such as a potential flow field within which the disturbances will decay with increasing height and become negligible before the surface is reached.

A step-by-step numerical study proceeding from streamline to streamline gives the shape and velocity distribution for the streamline at the upper edge of the shear layer (the lower edge of the potential flow field). Comparison of this velocity distribution with the correct distribution for that streamline shape in a potential flow field indicates the degree of compatibility with boundary conditions.

By changing the ratio of shear-layer thickness to disturbance wavelength and by altering the original simple shape of the stagnant region it is found that satisfactory examples can be obtained.

It is also found that the Richardson-number effects obtained originally for the simple shape apply to drastically modified shapes, subject to some minor restrictions.

Out of a large set of examples, then, a small subset appears to be consistent with the upper-boundary conditions, and we infer that this subset may be physically possible and exhibit the Richardson-number effects mentioned.

A crude check is made on the importance of circulation of the fluid, which has here been assumed stagnant.

3. Mathematical development

3.1. *Description of model*

The analysis is two-dimensional, with the streamwise co-ordinate x and the vertical co-ordinate z, $z = 0$ being at the level of the centre of the undisturbed shear layer (see figure 1). In the undisturbed state the density-stratified shear layer has zero velocity on the $z = 0$ axis. This separates flow to the right (above) from flow to the left (below).

In the disturbed state the blocked fluid is considered as trapped and mixed. For simplicity, zero velocity and uniform density are assigned to it (see figure 2). The disturbance is supposed periodic for some finite distance in the flow direction so that a half-cycle appears as in figure 2.

Inside the stagnant region a hydrostatic situation exists. Pressure P varies only with depth so that

$$P + \rho_{\mathrm{av}} g z = P'_0, \tag{1}$$

where ρ_{av} is the uniform density of the mixed region, P'_0 is the pressure at $z = 0$ and g is the acceleration due to gravity.

Above and below the stagnant region are streamlines extending to infinity in the streamwise direction. These obey the following equation:

$$P + \rho g z = -\tfrac{1}{2}\rho q^2 + \rho f_1(\rho), \tag{2}$$

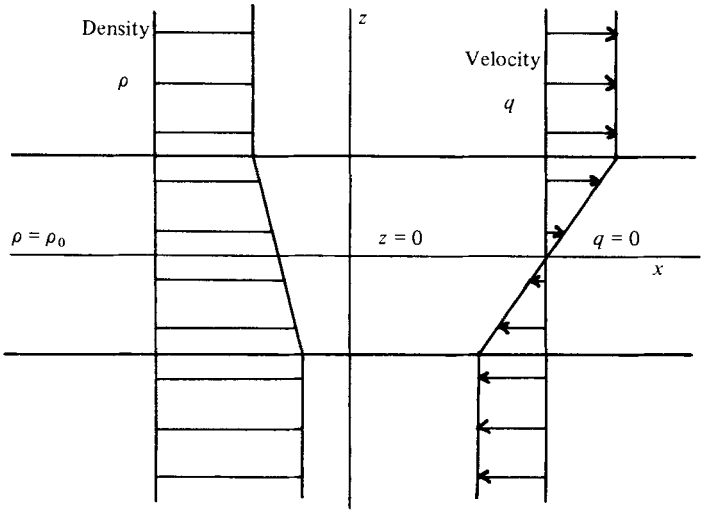

FIGURE 1. The undisturbed shear layer.

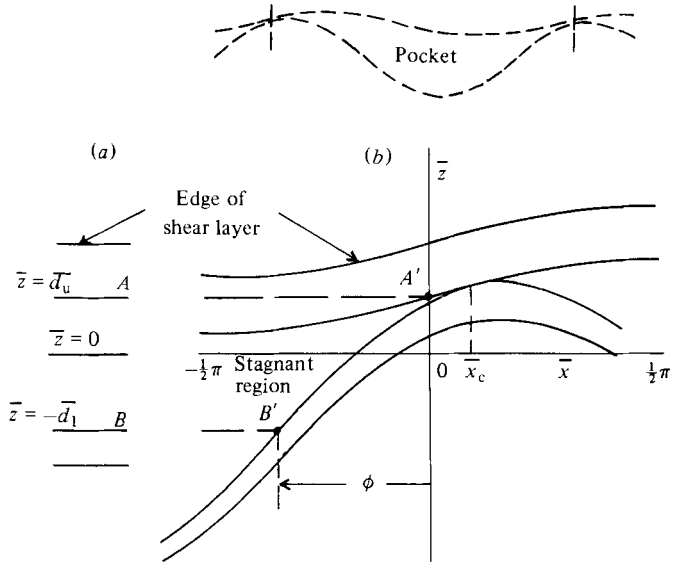

FIGURE 2. Stagnant region with phase displacement: (*a*) undisturbed flow; (*b*) disturbed flow. $\bar{P}$, $\bar{\rho}$, $\bar{q}$, $\bar{z}$ identical at A and A' and at B and B'.

where q is the local velocity. This is essentially equation (5), p. 21, in Lamb (1945). His Ω becomes gz and his C becomes a function of ρ, the density that identifies a particular streamline. (Density must be constant along any one streamline if the flow is to be steady.)

In addition continuity is defined by

$$dz'/d\rho = f_2(\rho)/q, \tag{3}$$

where z' is distance normal to the streamline. This says that stream-tube thickness is inversely proportional to velocity in this incompressible two-dimensional flow.

The functions $f_1(\rho)$ and $f_2(\rho)$ are assumed unaffected† by the process that disturbs the fluid and so can be determined from the velocity and density distributions specified for the initial undisturbed shear layer. These distributions are both assumed linear in z. Let $\rho = \rho_0 + \Delta\rho$, where ρ_0 is the density at $z = 0$ in the undisturbed shear layer. Then, with b and c constants,

$$q = bz, \quad \Delta\rho = -cz, \tag{4}$$

and f_1 and f_2 are defined by

$$\rho f_1(\rho) = P_0 + \tfrac{1}{2}\Delta\rho^2(\rho b^2/c^2 - g/c), \tag{5}$$

$$f_2(\rho) = (b/c^2)\,\Delta\rho. \tag{6}$$

P_0 is the pressure at $z = 0$ in the *undisturbed* shear layer, in contrast to P_0', which is the pressure at $z = 0$ in the stagnant region of the *disturbed* shear layer.

3.2. *Dimensionless variables*

It is convenient to make $\Delta\rho$ dimensionless by introducing $\overline{\Delta\rho}$, where

$$\overline{\Delta\rho} = \Delta\rho/\rho_0. \tag{7}$$

Specifying λ as the horizontal wavelength of the disturbance, with k the corresponding wavenumber, and q_i the velocity at the upper edge of the undisturbed shear layer, we have $\bar{x} = kx$, $\bar{z} = kz$, $\bar{q} = q/q_i$, $\bar{P} = P/\rho_0 q_i^2$, $\bar{b} = b/kq_i$, $\bar{c} = c/k\rho_0$, $B = \bar{b}/\bar{c}$ and $\bar{g} = g/kq_i^2$.

The Richardson number R, defined as $N^2/(dq/dz)^2$, where N is the Brunt–Väisälä frequency, becomes

$$R = \bar{g}/\bar{c}B^2. \tag{8}$$

3.3. *The stagnant region*

For simplicity this region is assumed bounded above and below by sine waves having the same wavelength but different amplitudes, $\bar{\alpha}$ and $\bar{\beta}$,‡ and different $\bar{x}$- and $\bar{z}$-origins (see figure 2). The upper boundary is given by

$$\bar{z} = \bar{\alpha}\sin\bar{x} + \bar{d}_u, \tag{9}$$

and the lower by

$$\bar{z} = \bar{\beta}\sin(\bar{x} + \phi) - \bar{d}_l, \tag{10}$$

where $\bar{x} + \phi = 0$ defines the inflection point for the lower sine wave. At $\bar{x}_c$, the contact point, the upper and lower boundaries must have the same $\bar{z}$ and the same $d\bar{z}/d\bar{x}$. $\bar{\beta}$ can be obtained by eliminating ϕ between the resulting equations,

$$\bar{\beta} = +[\bar{\alpha}^2 + 2\bar{\alpha}(\bar{d}_u + \bar{d}_l)\sin\bar{x}_c + (\bar{d}_u + \bar{d}_l)^2]^{\frac{1}{2}}. \tag{11}$$

Within the stagnant region the density is

$$\bar{\rho}_{av} = \tfrac{1}{2}(\bar{\rho}_u + \bar{\rho}_l), \tag{12}$$

and the pressure is

$$\bar{P} = \bar{P}_0' - \bar{\rho}_{av}\bar{g}\bar{z}. \tag{13}$$

† Outside the blocked thickness of the shear layer.

‡ Modifications of this shape are discussed later.

Here $\bar{\rho}_u$ and $\bar{\rho}_l$ are the densities of the upper and lower boundary streamlines. $\bar{P}'_0$ is $\bar{P}$ at $\bar{z} = 0$ in the stagnant region and is related to $\bar{P}_0$ (the pressure at $\bar{z} = 0$ in the undisturbed case) by

$$\bar{P}'_0 = \bar{P}_0 + \bar{g}|\overline{\Delta\rho_u}\,\overline{\Delta\rho_l}|/2\bar{c}. \tag{14}$$

The pressure at the upper boundary of the stagnant region is

$$\bar{P}_u = \bar{P}'_0 - \bar{\rho}_{av}\bar{g}(\bar{\alpha}\sin\bar{x} + \bar{d}_u), \tag{15}$$

and at the lower boundary

$$\bar{P}_l = \bar{P}'_0 - \bar{\rho}_{av}\bar{g}[\bar{\beta}\sin(\bar{x}+\phi) - \bar{d}_l]. \tag{16}$$

If in (15) $\bar{x}$ is zero then the pressure $\bar{P}$ is the same as on that streamline (identified by its density) in the undisturbed flow. The height $\bar{z}$ (see (9)) is also the same and therefore $\bar{q}$ is the same. This correspondence (and that for the lower boundary streamline) is indicated in figure 2.

3.4. *The boundary streamlines*

$\bar{P}$ must be continuous across the boundaries of the stagnant region, but the quantity $\overline{P+\rho gz}$, which is more convenient to use, is not continuous across the boundary. For the upper and lower streamlines this quantity is

$$\overline{(P+\rho gz)}_u = \bar{P}'_0 + (\bar{\rho}_u - \bar{\rho}_{av})\bar{g}[\bar{\alpha}\sin\bar{x} + \bar{d}_u], \tag{17}$$

$$\overline{(P+\rho gz)}_l = \bar{P}'_0 + (\bar{\rho}_l - \bar{\rho}_{av})\bar{g}[\bar{\beta}\sin(\bar{x}+\phi) - \bar{d}_l]. \tag{18}$$

Let $\bar{\rho}_u - 1 = \overline{\Delta\rho_u}$ etc., and let $|\overline{\Delta\rho_u}| = r$ and $|\overline{\Delta\rho_l}| = s$; then

$$\left.\begin{aligned} \bar{d}_u = r/\bar{c}, \quad \bar{d}_l = s/\bar{c}, \\ \bar{\rho}_u - \bar{\rho}_{av} = -\tfrac{1}{2}(r+s), \\ \bar{\rho}_l - \bar{\rho}_{av} = +\tfrac{1}{2}(r+s), \\ \bar{P}'_0 = \bar{P}_0 + \bar{g}rs/2\bar{c}. \end{aligned}\right\} \tag{19}$$

From (2) the velocities on the boundary streamlines are

$$\bar{q}_u = +\{\{-2[\overline{(P+\rho gz)}_u - \bar{P}_0] + r^2B^2(1-r-R)\}/(1-r)\}^{\frac{1}{2}}, \tag{20}$$

$$\bar{q}_l = -\{\{-2[\overline{(P+\rho gz)}_l - \bar{P}_0] + s^2B^2(1+s-R)\}/(1+s)\}^{\frac{1}{2}}. \tag{21}$$

The minimum velocity for the upper streamline occurs at $\bar{x} = -\frac{1}{2}\pi$ and for the lower at $\bar{x} + \phi = \frac{1}{2}\pi$. It is desirable to make each minimum velocity a fraction E of the undisturbed velocity (Br or $-Bs$) for the corresponding boundary streamline so that

$$\bar{q}_{um} = BrE, \quad \bar{q}_{lm} = -BsE, \tag{22}$$

where $0 < E < 1$. Then (20) and (21) with substitutions from (17), (18) and (19) can be put in the following forms:

$$(r^* + s^*)/(1-r) - r^{*2}(1-E^2)/R = 0, \tag{23}$$

$$(\bar{\beta}/\bar{\alpha})(r^* + s^*)/(1+s) - s^{*2}(1-E^2)/R = 0, \tag{24}$$

where the $*$ indicates division by $\bar{\alpha}\bar{c}$, and $\bar{\beta}/\bar{\alpha}$ can be obtained from (11). If $r^*+s^*=\xi^*$ and $r^*-s^*=\eta^*$ then the elimination of η^* (except in $1-r$ and $1+s$, which are $\simeq 1$) gives an equation defining ξ^* implicitly:

$$\xi^* = [R/(1-E^2)]^{\frac{1}{2}}\left\{\left[\frac{\xi^*}{1-r}\right]^{\frac{1}{2}}+\left[\frac{\xi^*}{1+s}(1+2\xi^*\sin\bar{x}_c+\xi^{*2})^{\frac{1}{2}}\right]^{\frac{1}{2}}\right\}, \tag{25}$$

with r^* and s^* defined by

$$\left.\begin{aligned} r^* &= [R/(1-E^2)]^{\frac{1}{2}}[\xi^*/(1-r)]^{\frac{1}{2}},\\ s^* &= [R/(1-E^2)]^{\frac{1}{2}}\left[\frac{\xi^*}{1+s}(1+2\xi^*\sin\bar{x}_c+\xi^{*2})^{\frac{1}{2}}\right]^{\frac{1}{2}},\\ \bar{\beta}/\bar{\alpha} &= [1+2\xi^*\sin\bar{x}_c+\xi^{*2}]^{\frac{1}{2}}. \end{aligned}\right\} \tag{26}$$

Suppose that the Richardson number R, the contact point $\bar{x}_c$ and the fraction E of the undisturbed velocity attained on the boundary streamlines are all specified. Then from (25) and (26) ξ^*, r^* and s^* can be found by iteration. Specifying the amplitude $\bar{\alpha}$ of the sine wave on the upper boundary of the stagnant region and the original density gradient $\bar{c}$ makes it possible to get r and s, which identify the boundary streamlines for the stagnant region. The entire geometry of the stagnant region is then known through (19) and (26), which give $\bar{d}_u$, $\bar{d}_l$ and $\bar{\beta}$.

From this geometry and (2) the starting conditions are obtained for step-by-step construction of the streamlines. However it is of more immediate interest to solve (25) for the Richardson number R and observe that, even in the most favourable case for large values ($\bar{x}_c = -\frac{1}{2}\pi$), the Richardson number cannot exceed unity.

4. Shape of the stagnant region

The preceding derivation depends on the minimum-velocity points and the contact point for the boundary streamlines, not on their precise shapes. For example, if the phase displacement is equal to π and the contact point is at $\bar{x} = -\frac{1}{2}\pi$, the minimum velocity points coincide with the contact point. The original upper sine wave can then be replaced by any curve which passes through the contact point, does not go below it and has a mean $\bar{z}$-value equal to $\bar{d}_u$. The lower sine wave can be altered with similar constraints, maintaining a mean $\bar{z}$-value of $-\bar{d}_l$. The amount of fluid in the stagnant region is then unchanged and the r- and s-values are unaltered from the sine-wave case. The step-by-step construction of streamlines then starts from these new boundaries and proceeds out to the edge of the shear layer. This procedure will be used later in studying the effect of shape changes on compatibility of the flow pattern with the outer potential flow regions.

It is also possible to derive equations similar to (23) and (24) for more general shapes using the minimum value of $\bar{z}_u$ ($\bar{z}_{u\,\min}$) and the maximum value of $\bar{z}_l$ ($\bar{z}_{l\,\max}$) instead of their specific values for sine waves.

It is necessary for $\bar{z}_{l\,\max}$ to be equal to or greater than $\bar{z}_{u\,\min}$ for a contact point to exist. Setting $\bar{z}_{l\,\max} = \bar{z}_{u\,\min} + C$, with C a positive constant, gives

$$-rs+(r+s)\bar{z}_{u\,\min}+r^2[(1-r)(1-E^2)/R-1] = 0, \tag{27}$$

$$-rs-(r+s)(\bar{z}_{u\,\min}+C)+s^2[(1+s)(1-E^2)/R-1] = 0. \tag{28}$$

Eliminating $\bar{z}_{u\,min}$ gives

$$R = \frac{(1-E^2)\,[r^2(1-r)+s^2(1+s)]}{(r+s)\,[r+s+C]}. \tag{29}$$

Let r and s be much less than unity and let E be 0. Then

$$R = (r^2+s^2)/[r^2+s^2+2rs+C(r+s)], \tag{30}$$

where r, s and C are all positive.

5. Richardson-number effects

If (25) is solved for the Richardson number R with r and s negligible (compared to unity),† it appears that R cannot exceed unity for the stagnant region with sine-wave boundaries. From (29) or (30) the same result is obtained for more general shapes.

Symmetry about a horizontal plane requires $\bar{\beta} = \bar{\alpha}$ and $\phi = \pi$, and r and s must be equal and much less than unity. The Richardson number must then be approximately one-half for sine-wave boundaries. Again, from (29) or (30) (with $C = 0$ for symmetry) the same result is obtained for more general shapes.

For Richardson number greater than $\frac{1}{2}$ (approximately) more than one solution can exist for a specified amplitude of the sine wave bounding the stagnant region above. This has not yet been explored.

If it is required that disturbances above and below the shear layer be of widely different magnitude then the Richardson number must approach unity for sinusoidal boundaries. The requirement that r and s be widely different in magnitude, with $C = 0$, brings a similar conclusion from (29) or (30) for more general shapes.

Richardson numbers greater than unity can be obtained by eliminating the requirement that there be contact points for the upper and lower boundaries of the stagnant region (letting C be negative in (29) and (30) is a sufficient condition). The pockets then merge to form a continuous stagnant layer which insulates flow above the critical height from flow below.

It is evident from the above that there is a strong dependence of the flow pattern on Richardson number in our analysis. Also, for high R, the critical level appears as a barrier to communication as it did in the quite different analysis of Booker & Bretherton (1967) based on mathematical developments by Miles (1961).

The modification of our stagnant region to include density stratification (instead of uniform density) might alter the picture somewhat. However we *conjecture* that an upper limit on Richardson number would exist also in that case for the following reasons. Portions of the constant-density stagnant region are maintained at levels above or below the levels consistent with that constant density in a completely static (undisturbed-flow) condition. The forces required to do this are produced dynamically by the curved flow in the surrounding shear layer. Even if the stagnant fluid is assumed to be stratified the density will vary only between the densities of the upper- and lower-boundary streamlines. Since these streamlines are not horizontal in disturbed flow, there are still portions of the stagnant region above or below the levels consistent with their densities. At high Richardson numbers density variation with height is large and velocity variation is small, so the dynamic forces available to support the

† r and s are less than 0·005 in the examples shown.

displaced stagnant region should become inadequate. Therefore, in the stratified case (as in the constant-density case), we *conjecture* that the type of flow pattern chosen would not exist for high Richardson numbers, and would break down to give a continuous stagnant insulating layer.

6. The shear-layer flow pattern

So far, only the stagnant region with its boundary streamlines has been examined. It is also necessary to construct the flow pattern throughout the shear layer to a potential-flow region above and to a potential flow region or a solid boundary below.

In (2) the velocity–pressure relation along any streamline is given. In (3) a continuity condition is given, and only a statement of the normal pressure gradient is now needed. This can be expressed in terms of the pressure gradients due to fluid weight and to centrifugal force. The latter depends on streamline curvature C_s. The normal pressure gradient is

$$dP/dz' = -\rho g \cos\theta - \rho q^2 C_s, \tag{31}$$

where z' is normal to the streamline, and θ, the streamline inclination to the horizontal, is

$$\theta = \arctan(dz/dx). \tag{32}$$

For convenience (31) can be rewritten as

$$d(P+\rho g z)/dz' = g z\, d\rho/dz' - \rho q^2 C_s. \tag{33}$$

A computer program for the step-by-step construction of streamlines was formulated using equations equivalent to (2), (3) and (33).

7. Potential-flow regions

Above the shear layer is a constant-density fluid which, in the undisturbed state, has a uniform horizontal velocity equal to that at the top of the undisturbed shear layer. The thickness of this potential-flow region is assumed much larger than the horizontal wavelength of the disturbance, and the disturbance is to decay exponentially with increasing height in this region. In order that it should do so, the velocity distribution along the streamline at the edge of the shear layer must have a special relation to the streamline shape. Whatever streamline shape appears at the upper edge of the shear layer is matched (approximately) by a streamline in potential flow. This is accomplished by representing the potential-flow stream function ψ as a summation of terms, each harmonic in x and exponential in $-z$, and adjusting the coefficients to give good shape agreement. The velocity distributions along the original and matching streamlines are then compared. If these are 'reasonably' close the example is accepted as being compatible with the potential flow. Otherwise the example is rejected. Alteration of the ratio of shear-layer thickness to wavelength seems to be the most effective way of obtaining the desired total variation of velocity along the streamline. Alteration of the shape of the stagnant region is necessary to get a more precise agreement.

Below the shear layer it is only necessary to replace some streamline by a solid surface and say that this contour is generating the entire disturbance.

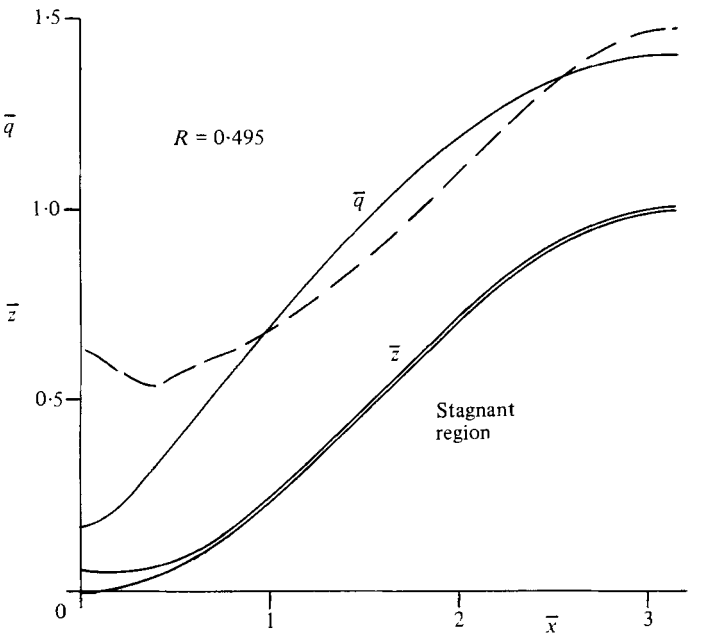

FIGURE 3. Example (1): stagnant region bounded by sine waves. Potential flow, — —.

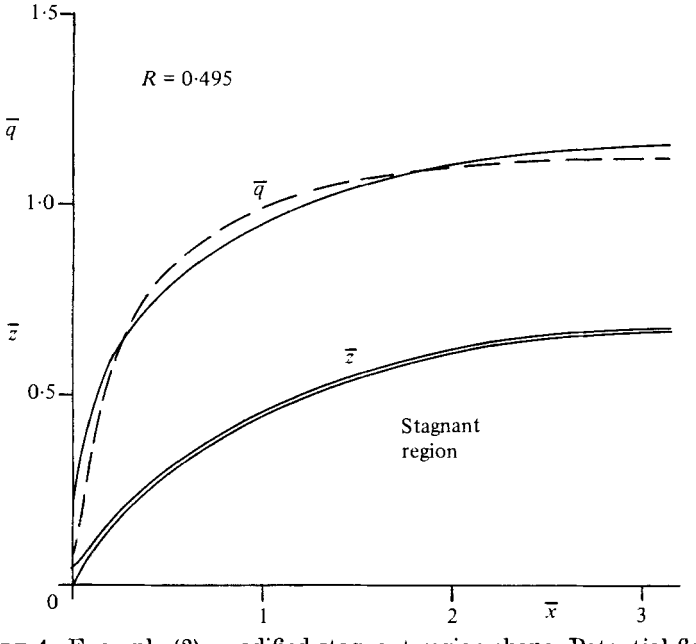

FIGURE 4. Example (2): modified stagnant-region shape. Potential flow, — —.

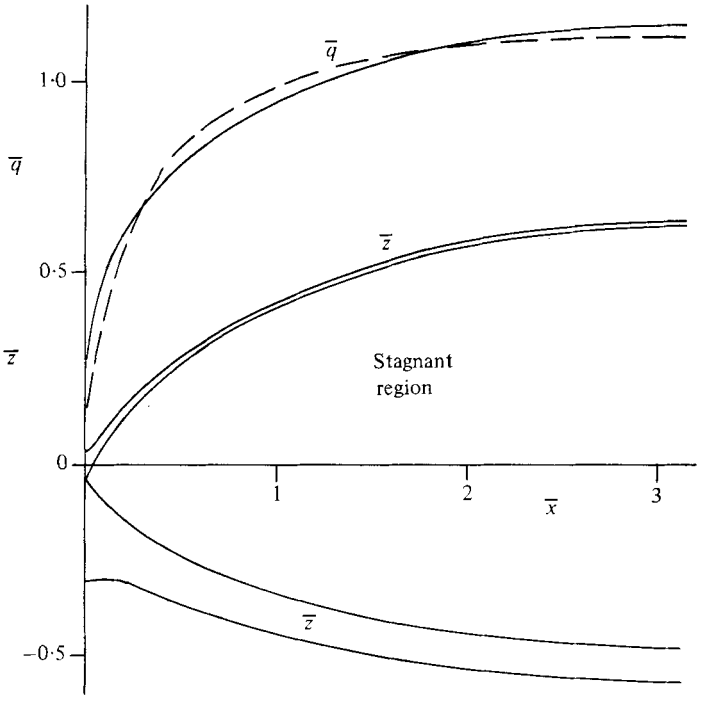

FIGURE 5. Example (3): $R = 0{\cdot}5$. Potential flow, — —.

8. Examples

Specification of the Richardson number R, the contact point $\bar{x}_c$, and the smallest fraction E of the undisturbed velocity measured on the boundary streamlines allows one to solve (25) for ξ^* and then get the geometry of the stagnant region as described in § 3.4. However, for R very close to 0·5 there are three values of ξ^* satisfying (25). Below this there is only one value and above there are two roots. The roots will be labelled first, second and third, taken in the order of increasing ξ^*.

Examples (1) and (2) (figures 3 and 4) use the second root and are chosen to illustrate the degree of compatibility attained between the inner flow and the potential flows outside the shear layer. The flow pattern is almost symmetrical top to bottom. This required adjusting the Richardson number to 0·495, since the relation between upper and lower flow patterns is sensitive to R in the neighbourhood of $R = 0{\cdot}5$. For example (1) the stagnant region is bounded by sine waves. The fractional density change $2m$ across the shear layer is 0·01, the shear-layer thickness over the disturbance wavelength, t, is 0·16, and E, the ratio of the minimum velocity on a bounding streamline to the undisturbed velocity of the streamline, is 0·1. The thickness parameter t was chosen to give the correct magnitude of velocity change at the edge of the shear layer.

In example (2) the stagnant region is bounded by streamlines of modified shape (a portion of an ellipse) with the above parameters unchanged. Figures 3 and 4 show the shape of one half-cycle of the upper half of the stagnant region (note exaggeration of the vertical scale), the shape of the streamline at the edge of the shear layer, and the velocity distribution along that streamline. For comparison, the velocity distribution

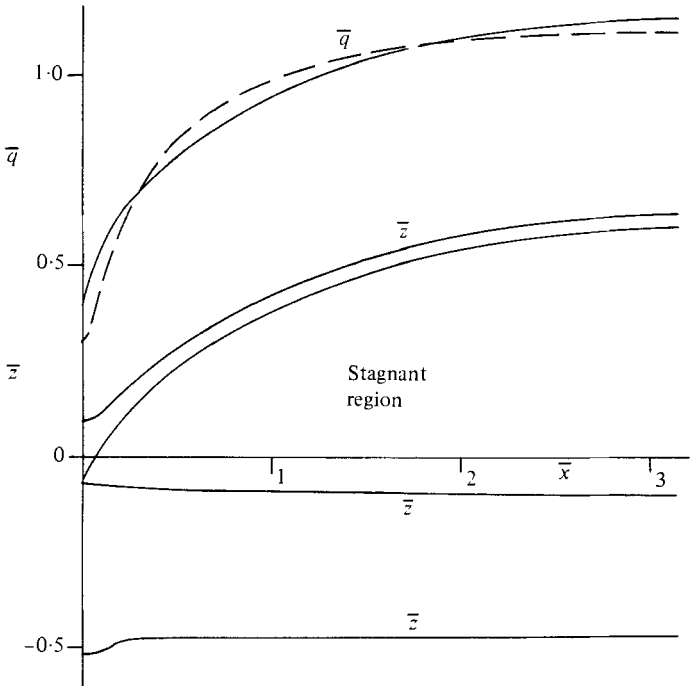

FIGURE 6. Example (4): $R = 0{\cdot}7$. Potential flow, — —.

which would exist on that streamline in a potential flow is shown. (The accuracy of the numerical methods used is questionable in the $\bar{x}$-interval from 0 to $\frac{1}{8}\pi$.) It is clear that example (2) shows better detailed agreement in this velocity comparison, although example (1) has almost the correct trend except in the region $\bar{x} = 0$ to $\bar{x} = \frac{1}{8}\pi$. Further improvement in the velocity comparison might be expected from a thorough study of shapes.

Examples (3)–(5) at Richardson numbers of 0·5, 0·7 and 0·9 (figures 5–7) are chosen to show the behaviour of the flow pattern as R approaches unity. The thickness parameter t varies from 0·15 to 0·18 in this series, being adjusted to get better potential-flow agreement at the upper edge of the shear layer. Other parameters† are the same as in examples (1) and (2). The stagnant-region shapes are all elliptic arcs, and the agreement with potential flow at the upper edge of the shear layer is comparable to that in example (2).

Comparison of example (3) at $R = 0{\cdot}5$ with example (2) at $R = 0{\cdot}495$ shows the sensitivity to Richardson number in the neighbourhood of $R = 0{\cdot}5$.

Examples (4) and (5) show the tendency for disturbances above and below the critical layer to vary greatly in magnitude at high Richardson number (by a factor of 22 at $R = 0{\cdot}7$ and a factor of 436 at $R = 0{\cdot}9$). These flow patterns can be inverted (almost exactly) so the larger disturbance can be either above or below. This difference in magnitude might be interpreted as the approach to complete independence which, in the absence of rotational effects, is finally realized for $R > 1$. The upper and lower patterns are then separated by a continuous stagnant layer.

† The second root is used in this series also.

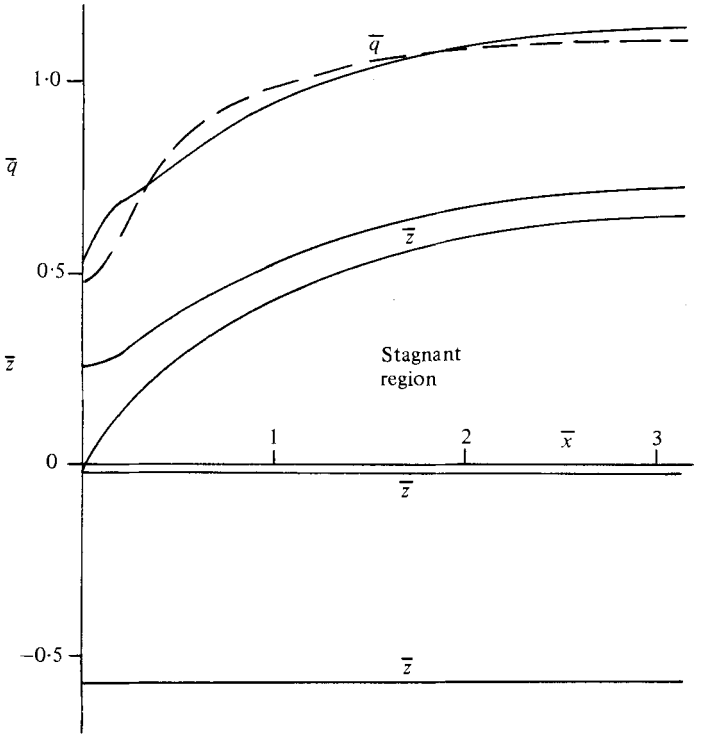

FIGURE 7. Example (5): $R = 0{\cdot}9$. Potential flow, — —.

Cases using the first root, with Richardson numbers 0·5, 0·7 and 0·9 (not illustrated here), show a trend similar to examples (3)–(5).

A case with $R = 0{\cdot}3$ was also studied (but is not included here). The value of t was adjusted to 0·08 for potential-flow agreement. The upper amplitude was $3\frac{1}{2}$ times greater than the lower, but this contrast is small compared to the factors of 22 and 436 obtained for $R = 0{\cdot}7$ and $R = 0{\cdot}9$ respectively.

Cases with phase displacement have not been studied sufficiently for presentation here.

Non-uniqueness

The shape of the lower portion of the stagnant region could perhaps be adjusted to fit a potential flow below.† However, we have chosen to consider a rigid wavy boundary below, which can (within our assumptions) support any pressure or velocity distribution. Adjustment of the lower-stagnant-region shape can then provide, for a fixed upper flow, an infinite family of lower flows, each bounded by its own rigid wavy wall with its own pressure distribution. Our theory is not sufficiently sophisticated to exclude such an infinite family of flows, which might actually be restricted by rotational effects or by stability considerations. Margolis & Su (1978) also note non-unique solutions.

† I.e. if the value of t required is not incompatible with the value required for the upper side.

9. Rotational effects

In this analysis the fluid in the pockets has been assumed stagnant. Actually some rotation or circulation must be created by the action of viscous forces, so that the pocket resembles a single eddy. Centrifugal forces due to rotation may compensate partially for the static imbalance of pressures (which exists because the uniform-density pocket is not in equilibrium with the undisturbed stratified fluid). Rotational velocities are controlled by velocities on the boundary streamlines, and flow curvatures are estimated from the curvature of the boundary streamlines. On this basis a crude estimate of the ratio of centrifugal force to the force from static imbalance is made. This gives a factor of importance F_R for rotational effects which is

$$F_R = [\pi^2/2R][(r+s)t/2m]^2.$$

Here $(r+s)t/2m$ measures the ratio of the blocked shear-layer thickness to the disturbance wavelength (or the ratio of mean amplitude to wavelength for the disturbance).

If F_R approaches zero the rotational effects are negligible. If $F_R = 1$ the full static imbalance could be supported by the centrifugal force and the assumption of stagnant fluid in the pockets is inadequate. In the examples shown, F_R ranges from 0·03 to 0·24 approximately.

10. Conclusions

(1) Alterations of the ratio of shear-layer thickness to disturbance wavelength and of the shape of the stagnant region boundaries can bring acceptable agreement with the potential flow-field boundary conditions.

(2) The primary Richardson-number effects are independent of the stagnant region shape.

(3) The analysis shows strong Richardson-number effects as follows.

(*a*) The flow pattern breaks down to give a continuous stagnant insulating layer for Richardson numbers greater than unity.†

(*b*) Flow patterns almost symmetrical about the critical height exist for Richardson numbers near $\frac{1}{2}$.

(*c*) Large amplitude differences above and below the critical height can exist for Richardson numbers slightly less than unity.

(4) For Richardson numbers greater than $\frac{1}{4}$ the omission of rotational effects seems justifiable if the disturbance amplitude is not too large a fraction of the disturbance wavelength.

(5) It is not yet clear what steady-state flow pattern exists for an example with a ratio of shear-layer thickness to disturbance wavelength which does not allow the boundary conditions to be satisfied.

† This restriction applies even if the blocked region extends outside the shear layer.

REFERENCES

BENNEY, D. J. & KO, D. R. S. 1978 The propagation of long large amplitude internal waves. *Stud. Appl. Math.* **59**, 187–199.

BOOKER, J. R. & BRETHERTON, F. P. 1967 The critical layer of internal gravity waves in a shear flow. *J. Fluid Mech.* **27**, 513–539.

BRETHERTON, F. P. 1966 The propagation of groups of internal gravity waves in a shear flow. *Quart. J. Roy. Met. Soc.* **92**, 466–480.

HINES, C. O. & REDDY, C. A. 1966 On the propagation of atmospheric gravity waves through regions of wind shear. (Unpublished.)

KELLY, R. E. & MASLOWE, S. A. 1970 The nonlinear critical layer in a slightly stratified shear flow. *Stud. Appl. Math.* **49**, 301–326.

LAMB, H. 1945 *Hydrodynamics*. Dover.

MARGOLIS, S. B. & SU, C. H. 1978 Boundary-value problems in stratified shear flows with a nonlinear critical layer. *Phys. Fluids* **21**, 1247–1259.

MASLOWE, S. A. 1972 The generation of clear air turbulence by nonlinear waves. *Stud. Appl. Math.* **51**, 1–16.

MASLOWE, S. A. 1973 Finite-amplitude Kelvin–Helmholtz billows. *Boundary-Layer Met.* **5**, 43–52.

MILES, J. W. 1961 On the stability of heterogeneous shear flows. *J. Fluid Mech.* **10**, 496–508.

MOLLO-CHRISTENSEN, E. 1978 Gravitational and geostrophic billows: some exact solutions. *J. Atmos. Sci.* **35**, 1395–1398.